EXPERIMENTAL ANALYSIS OF MICROPARTICLES BEHAVIOUR IN MICROCAVITIES

Vilkinis P.*, Šereika J., Skarbalius G., Džiugys A., Pedišius N.
*Author for correspondence
Laboratory of Heat-Equipment Research and Testing,
Lithuanian Energy Institute,
Kaunas, LT-44403,
Lithuania,
E-mail: paulius.vilkinis@lei.lt

ABSTRACT

Precise control of microscale fluid flow plays a significant role in biotechnology applications. Microfluidics structures, such as microcavities, have been widely applied in various biomedical, biochemical, and high-throughput screening applications. However, the particles trapping mechanism into microchannels are not fully understood yet and demands further research. Particles separation and trapping can be performed using various techniques. In the present work, investigations are focused on inertial microfluidics. Hydrodynamic forces, such as wall-induced and shear-induced lift forces, are employed to control particle behaviour in the microcavities.

In this work, the capabilities to trap microparticles in rectangular microcavities with rounded bottom corners are investigated experimentally. Also, microparticles' behaviour in the microchannels and microcavities are analyzed depending on cavity geometry and Re number. A Series of experimental investigations are performed at different Re numbers to determine threshold values of particles that are trapped in a micro vortex and pass microcavity without trapping. Also, the behaviour of microparticles is related to the flow structure in the cavities. Therefore, flow fields obtained by micro-PIV equipment are used to ascertain flow structure influence on particle behaviour. Fundamental knowledge and its generalization of particle trapping and overall behaviour regularities depending on controlling parameters, such as geometry and flow regime, will serve as a roadmap to aid the development of the optimal design of micro-and nanofluidic devices. This study extends the research area of flow dynamics in microcavities where shear layer growth is caused by the interaction of separated and recirculated flows.

INTRODUCTION

Particle separation and trapping has been extensively studied for more than a decade in various science fields, such as biomedicine, chemistry, electronics industry, etc. In microfluidics, microscale structures have been used in various lab-on-chip and micro-total-analysis systems where cell trapping and separation play a major role [1–3]. One of the main science fields which requires cell trapping method improvements is the biomedicine. Much attention is paid to trapping, docking, and size-based separation of cells and particle problems [4]. The separation of particular cells from biological samples is critical in clinical applications for subsequent diagnosis and analysis. Isolating certain rare circulating cells from blood samples, such as circulating tumour cells (CTCs) [5], is mandatory to use these cells as clinical indicators. Microparticle trapping occurs in practical applications such as lymphocyte separation for blood to perform HIV tests, stem cell enrichment, or disease detection. Particle separation and trapping can be performed using various techniques; therefore, the present investigation is focused on inertial microfluidics.

Hydrodynamic trapping is usually applied to separate the target particle from the main flow utilizing barriers, obstructions, or cut-outs in microchannels. Inertial forces focus on different-sized particles at different locations where they can be selectively separated. Zhou et al. [6] investigated particle trapping in micro vortices mechanism by changing the size of the trapping region, particle concentration, and flow parameters. The authors found that trapping is dictated by Re number, which exceeds the threshold value that triggers the particle in the vortices. Also, particle trapping and separation processes depend on external disturbances such as pulsating flow [7]. Therefore, it has a positive influence on the liberation of particles that were trapped in vortices. Usually, simple square or rectangular open-type cavities shapes are employed. Park et al. [8] investigated the influence of microcavity shaping the ability to trap a single cell. It was shown that the equilateral triangle shape provides the best results because it has the strongest recirculation pattern in the microcavity. However, simulations were performed only at very low Re numbers, and it remains unclear how particle behaviour changes in different shapes of cavities at higher flow rates. Dhar et al. [5] demonstrated that cell trapping in the microcavities might be controlled by changing channel dimensions before the cavity. Narrowing the entry channel leads to higher trapping efficiency. The single-particle behaviour inside microcavity was studied by Shen et al. [9]. The authors concluded that particle orbit depends on the size and density of the particle and affects trapping and sorting in the cavity. In their later study, Shen et al. [10] investigated the influence of microcavity trailing walls on the trapping behaviours of a single particle. The authors determined three different trapping phenomena depending on the cavity aspect ratio and flow conditions. It was experimentally shown that particle trapping behaviour depends

on particle dynamics and micro vortex structure, which depends on microcavity geometry. In this study, the authors changed the only length of the cavity while width and depth were fixed.

This study aims to investigate flow structure and particle behaviour in semi-circular cavities depending on cavity length-to-depth ratio and Re number. Flow structure is experimentally analyzed using the micro-PIV method, and particle tracking velocimetry is employed to investigate particle movement in cavities. Particles' behaviour is associated with flow structure, and guidance for passive control of particles in the cavity are presented.

MATERIALS AND METHODS

Flow structure measurements in the cavity are performed using micro-particle image velocimetry (μPIV) system. Experimental measurements were conducted in microchannels with cavities varying in length and depth. The channel chip is made from Plexiglass (PMMA). The channel is of rectangular cross-section with width 0.9 mm and height h = 0.4 mm. Semi-circular cavities are located on both sides of the channel. Four different cavities' length-to-depth ratios, namely, 1, 1.3, 1.67 and 2, are chosen for investigation.

The μPIV system provided by Dantec Dynamics consists of double pulsed neodymium-doped yttrium aluminium garnet (Nd: YAG) laser (λ = 532 nm), laser control system LPU 450, FlowSense EO CCD camera providing an image field of 2048 × 2048 pixels mounted on the inverted Leica DM ILM microscope. The microscope is equipped with a dichroic mirror used to filter out background noise, and only florescent light from excited tracer particles can reach the camera. 1 μm diameter tracer particles (Invitrogen) with a specific gravity of 1.05 were used, with particles excitation and emission wavelengths of 535 nm and 575 nm, respectively. The fluid flow is generated with Elveflow OB1MK3 pressure controller ensuring inlet pressure up to 8 bar(g).

Neutrally buoyant polystyrene 20 μm in diameter particles are used in this work for particle behaviour investigations. Particles are mixed in deionized water, a 1 % v/v of Tween 20 is added to avoid particle coagulation and channel clogging. DynamicStudio software is used to analyze PIV data; additionally. The image pairs of tracer particles were captured at 15 Hz frequency with the time interval in the image frames varied from 5×10^{-3} s to 1×10^{-5} s depending on the flow rate. Time-averaged velocity data were obtained by averaging flow images for at least 10 s of flow. An adaptive correlation lgorithm was applied for image processing. A spatial esolution of 20.6 μm × 20.6 μm and depth of correlation of 42.4 μm were achieved. ImageJ is employed to perform particles tracking.

RESULTS AND DISCUSSION

Flow structure in the cavity

A series of flow fields measured in the mid-plane of cavities are shown in Fig. 1. The results displayed correspond to different cavity length-to-depth ratios changing from 1 to 4 and four different Re numbers. As it can be seen, flow in the cavities features three distinctive flow patterns depending on Re, namely attached, transitional, and separated flow. Such flow structure classification is prevalent in this type of research [9,11]

In the case of a short and deep cavity (L/h = 1), a recirculation zone is formed in the cavity throughout the whole Re range. At low Re, the vortex is small and located at the bottom of the cavity. As Re increases, the vortex grows larger and gradually fills the whole cavity. At Re = 100, the vortex is already reached size. As Re further increases, only the vortex centre changes its location, shifting slightly downstream. As the cavity size increases to L/h = 2, the recirculation zone is absent in the cavity; thus, the flow is attached. As Re increases up to Re = 10, a small recirculation zone is formed behind the leading edge of the cavity. The flow topology contains both separated and attached flow features; therefore, flow topology is called transitional. At Re = 100 and Re = 1000, whole cavity is filled with recirculation zone. In this case, the shift of the vortex centre from the vicinity of the leading cavity edge to the trailing edge is clearly visible. The shift is determined by higher kinetic energy transfer from the shear layer to the recirculation zone due to higher flow velocity. Similar flow topology is observed in L/h = 3 and L/h = 4 cases. It should be noted that particles can be trapped only in a separated flow case. In the case of attached flow, particles simply follow streamlines and leave the cavity. In the case of transitional flow, particles may be trapped in the recirculation zone, but after several rotations around the vortex centre, the particle leaves the cavity [9].

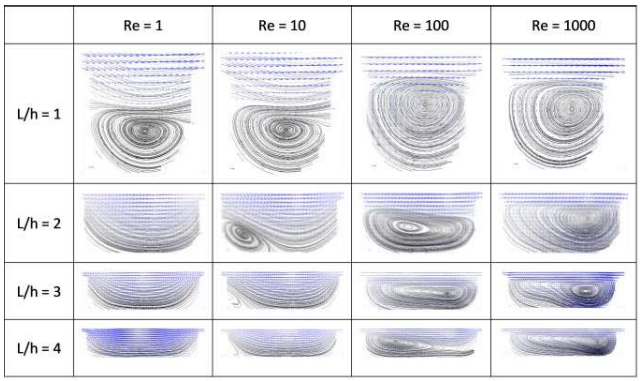

Fig. 1. Flow fields in the rectangular cavity at different length-to-depth ratios and Re numbers

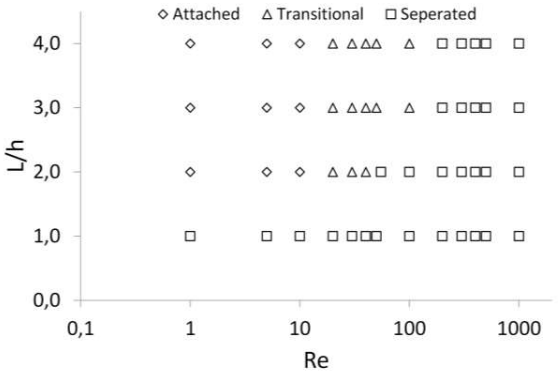

Fig. 2. Phase diagrams of the cavity flow topology regimes of rectangular cavities

Particle behaviour in cavities

Stokes number for particles immersed in water is Stk>> 1; therefore, particles follow flow streamlines and may be trapped in recirculation zones. Visualized particles' tracks are presented in Fig. 3. Instantaneous particles images over 1-2 seconds of flow are stacked together, thus visualizing particle patches. Cases of Re = 10 and 200 are presented in Fig. 3. Due to limited equipment capabilities, particle tracing at a higher Re number couldn't be performed. Selected Re numbers cover attached, transitional and separated flow regimes in different cavities cases.

In the case of L/h = 1, at Re = 10 (Fig. 3a), particles enter the cavity and follow a single streamline in the recirculation zone. The particle enters the cavity at the edge of the cavity's trailing edge. However, it can be seen that the particle leaves the cavity at the trailing edge after a single rotation in the cavity. As Re number increases (Fig. 3b), additional particle orbit is observed in the vicinity of the vortex centre. Also, a thicker outside orbit indicates more particles falling into the recirculation zone. Measured particle patch correlates well with results presented by Shem et al. [9] and Zhou et al. [6].

In the case of L/h = 2, at Re =10 (Fig. 3c) it is clear that particles follow streamlines. Most of the particle bridges the cavity without entering deep into the cavity. Also, weak contours of the vortex located behind the leading edge of the cavity are observed. Considering blurred contours of the corner vortex, it could be stated that only few particles are attracted into the vortex and stay in it for a short duration. Interestingly, no particles are observed in the cavity at Re = 200 (Fig. 3d). The time required for lateral migration may be too short at given Re [6]. Conversely, particles enter the cavity in the case of L/h = 1 (Fig. 3b) at the same Re; however, a vortex is stronger in the smaller cavity; therefore, shear lifting lateral force may be stronger and sufficient to attract particles into the cavity [6].

As cavity length increases to L/h = 3 and L/h = 4, it could be seen that particles precisely follow streamlines. As the small vortex behind a leading cavity wall is weak (Fig. 3 e and g), only a small number of particles are attracted to it and leave it promptly, as blurry vortex contours indicate. At higher Re (Fig. 3 f and h), particles are trapped in the cavity, indicating a clear particle patch overlapping with flow streamlines. However, the particle path leading out of the cavity at the trailing edge of the cavity is visible in the case of L/h = 4 at Re = 200 (Fig. 3h), indicating that particle trapping is not permanent.

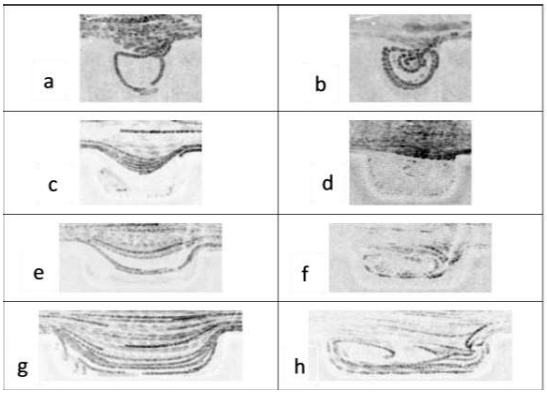

Fig. 3. Particles patches in cavity at different Re a) L/h = 1, Re = 10; b) L/h = 1, Re = 200; c) L/h = 2, Re = 10; d) L/h = 2, Re = 200; e) L/h = 3, Re = 10; f) L/h = 3, Re = 200; g) L/h = 4, Re = 10; h) L/h = 4, Re = 200

CONCLUSIONS

In this study, flow topology in rectangular cavities with different length-to-depth ratios in the range of L/h = 1–4 and a wide Re range of Re = 1–1000 was investigated experimentally. Additionally, the behaviour of 20 μm particles in cavities was studied, along with the cavities' ability to trap particles inside the recirculation zone was studied in Re number range of 10 -200.

Three distinctive flow regimes, namely attached, transitional and separated, are observed in cavities depending on the length-to-depth ratio and Re. Flow topology generalization depending on geometry and flow regime, is anticipated to serve as a valuable roadmap to help design particles trapping applications.

It was shown that 20 μm diameter microparticles follow streamlines in the cavity. In most cases, particles are attracted into the recirculation zone; however, permanent particle tracking was not observed. Instead, particles leave the cavity after turning around the vortex centre several times or leave the measurement plane due to the transverse velocity component.

FUNDING

This research was funded by Research Council of Lithuania; grant number S-MIP-21-21.

REFERENCES

[1] J. Yin, J. Deng, C. Du, W. Zhang, X. Jiang, Microfluidics-based approaches for separation and analysis of circulating tumor cells, TrAC - Trends Anal. Chem. 117 (2019) 84–100. https://doi.org/10.1016/j.trac.2019.07.018.

[2] M. Antfolk, S.H. Kim, S. Koizumi, T. Fujii, T. Laurell, Label-free single-cell separation and imaging of cancer cells using an integrated microfluidic system, Sci. Rep. 7 (2017) 1–12. https://doi.org/10.1038/srep46507.

[3] D. Yang, F. Gao, Q.-T. Cao, C. Wang, Y. Ji, Y.-F. Xiao, Single nanoparticle trapping based on on-chip nanoslotted nanobeam cavities, Photonics Res. 6 (2018) 99. https://doi.org/10.1364/prj.6.000099.

[4] J. Nilsson, M. Evander, B. Hammarström, T. Laurell, Review of cell and particle trapping in microfluidic systems, Anal. Chim. Acta. 649 (2009) 141–157. https://doi.org/10.1016/j.aca.2009.07.017.

[5] M. Dhar, J. Wong, A. Karimi, J. Che, C. Renier, M. Matsumoto, M. Triboulet, E.B. Garon, J.W. Goldman, M.B. Rettig, S.S. Jeffrey, R.P. Kulkarni, E. Sollier, D. Di Carlo, High efficiency vortex trapping of circulating tumor cells, Biomicrofluidics. 9 (2015). https://doi.org/10.1063/1.4937895.

[6] J. Zhou, S. Kasper, I. Papautsky, Enhanced size-dependent trapping of particles using microvortices, Microfluid. Nanofluidics. 15 (2013) 611–623. https://doi.org/10.1007/s10404-013-1176-y.

[7] H. Başağaoğlu, J.T. Carrola, C.J. Freitas, B. Başağaoğlu, S. Succi, Lattice Boltzmann simulations of vortex entrapment of

particles in a microchannel with curved or flat edges, Microfluid. Nanofluidics. 18 (2015) 1165–1175. https://doi.org/10.1007/s10404-014-1509-5.

[8] J.Y. Park, M. Morgan, A.N. Sachs, J. Samorezov, R. Teller, Y. Shen, K.J. Pienta, S. Takayama, Single cell trapping in larger microwells capable of supporting cell spreading and proliferation, Microfluid. Nanofluidics. 8 (2010) 263–268. https://doi.org/10.1007/s10404-009-0503-9.

[9] F. Shen, M. Xu, Z. Wang, Z.M. Liu, Single-particle trapping, orbiting, and rotating in a microcavity using microfluidics, Appl. Phys. Express. 10 (2017). https://doi.org/10.7567/APEX.10.097301.

[10] F. Shen, S. Xue, M. Xu, Y. Pang, Z.M. Liu, Experimental study of single-particle trapping mechanisms into microcavities using microfluidics, Phys. Fluids. 31 (2019). https://doi.org/10.1063/1.5081918.

[11] R. Fishler, M.K. Mulligan, J. Sznitman, Mapping low-Reynolds-number microcavity flows using microfluidic screening devices, Microfluid. Nanofluidics. 15 (2013) 491–500. https://doi.org/10.1007/s10404-013-1166-0.